EUROPEAN FUSION DEVELOPMENT AGREEMENT

EFDA–JET–CP(03)01-67

A. Huber, P. Coad, G. Corrigan, L. C. Ingesson, K. Itami, S. Jachmich,
A. Korotkov, G.F. Matthews, Ph. Mertens, V. Philipps, R. Pitts, J. Rapp,
B. Schweer, G. Sergienko, M. Stamp, M.Wischmeier
and JET EFDA Contributors

Tomographic Reconstruction of 2-D Line Radiation Distribution in the JET MkIIGB Divertor in Pure He and D Discharges

Tomographic Reconstruction of 2-D Line Radiation Distribution in the JET MkIIGB Divertor in Pure He and D Discharges

A. Huber[1], P. Coad[2], G. Corrigan[2], L. C. Ingesson[3], K. Itami[4], S. Jachmich[1], A. Korotkov[2], G.F. Matthews[2], Ph. Mertens[1], V. Philipps[1], R. Pitts[5], J. Rapp[1], B. Schweer[1], G. Sergienko[1], M. Stamp[2], M.Wischmeier[5]
and JET EFDA Contributors*

[1]Institut für Plasmaphysik, Forschungszentrum Jülich GmbH, EURATOM Association, Trilateral Euregio Cluster, D-52425 Jülich, Germany,
[2]EURATOM/UKAEA Fusion Association, Culham Science Centre, Abingdon,OX14 3DB, UK
[3]FOM-Instituut voor Plasmafysica, Nieuwegein, The Netherlands,
[4]Japan Atomic Energy Research Institute, Naka-machi, Ibaraki-ken, Japan 311-0193,
[5]CRPP, Association EURATOM-Confederation Suisse, EPFL, Lausanne, Switzerland
**See Annex of J. Pamela et al., "Overview of Recent JET Results and Future Perspectives", Fusion Energy 2000 (Proc. 18th Int. Conf. Sorrento, 2000), IAEA, Vienna (2001).*

Preprint of Paper to be submitted for publication in Proceedings of the
EPS Conference on Controlled Fusion and Plasma Physics,
(St. Petersburg, Russia, 7-11 July 2003)

ABSTRACT.
Comparison of equivalent Helium and Deuterium discharges can supply important information for a deeper understanding of impurity sources and radiation characteristics in the divertor region. In a He plasma, a significantly different impurity release and its radiation behaviour is expected, which has a strong impact on divertor physics, modifying the character of detachment and density limits. When compared to Deuterium plasma the L-mode density limit in Helium is approximately twice as high (1.4 times the Greenwald limit) [1].

1. EXPERIMENTAL SETUP

At JET, the spatial distribution of impurity radiation in the divertor has been analysed using three CCD cameras coupled to selectable interference filters (D_α, CII-, CIII-, HeI-, HeII- emission lines). These measurements were obtained in Helium and Deuterium L-mode density ramp discharges and a 3D-tomographic reconstruction [2] reduced to a 2D-problem by the assumption of toroidal symmetry has been performed. In addition to the line-resolved spatial distributions from CCD cameras, distributions of total radiated power from bolometry are also available.

2. RESULTS AND DISCUSSION

L-mode 'density limit' experiments have been performed with $B_T = 2.4$ T, $I_P = 2$ MA and with an additional NBI power of 2.3-3.0MW. Figure 1 shows the time evolution of a typical deuterium (left) and helium (right) L-mode density limit discharges in JET with the MkIIGB divertor. The plasma density in both cases was raised steadily to the density limit by gas fuelling at constant input power. In D-plasma the integral ion flux to the outer divertor, measured by an array of Langmuir probes, initially increases, while the flux to the inner divertor remains low with continuously decrease until the discharge disruption. This indicates that the inner divertor is detached from the start. But Da emission in the inner divertor and neutral pressure in the divertor chamber (not shown) continue to increase. This is the signature of plasma detachment [3], which is characterised by a substantial drop both in particle and energy fluxes to the target plates, as well as in the pressure along the magnetic field lines. In He-plasma (Fig.1 on the right) the behaviour of detachment is totally different. In early phase of discharge, the inner target ion flux slightly increases and after reaching of density of $4\text{-}4.5\times10^{19}$ m^{-3} begin to decrease. In D-plasma shortly before discharge disrupts, a MARFE forms which leads to a 'density limit' disruption (70-80% radiative power fraction). In helium, the density can be increased without inner wall MARFE forming up to 100% radiative power fraction, which happens to be at much – by more than 70% – higher density (8.6×10^{19} m^{-3}). A general comparison of scrape-off layer and divertor physics in pure He and D discharges is given in [4]. Let us analyse the atomic physics and recycling properties of He and D, since those can be responsible for the differences in the detachment behaviour:

VOLUME RECOMBINATION

Around 1.3eV for D and 2.2eV for He, the ionisation and recombination rate coefficients are approximately equal [5]. For this temperatures, the recombination rate coefficients are relatively low

(2×10^{-18} m^3 s^{-1} for D and 1×10^{-18} m^3 s^{-1} for He [5]), so that for $n_e = 5\times10^{19}$ m^{-3}, the characteristic times for recombination are 10ms and 20ms. It is comparable to or longer than the ion transit time in the divertor for a flow speed of ~10^4m/s. There is thus in both cases no sufficient time for volume recombination to occur. The measured ratios D_γ/D_α and HeI (492nm)/HeI(502) (see lower graphics in the Fig.1) are below 0.03 and 1.6 respectively. If the whole radiation is caused by recombination, the D_γ/D_α and HeI (492nm)/HeI(502nm) ratios must be about 0.12 and 4 respectively [5], confirming that the major contributing process to emissions in inner and outer divertor is excitation. Probably another recombination process associated with excited hydrogen molecules, so called molecular activated recombination (MAR) plays a substantial role at least in early phase in the divertor detachment. For $T_e = 3$eV and $n_e = 1\times10^{19}$ m^{-3}, the rate is about factor of 1000 larger than the volume recombination rate and is about 2×10^{-16} m^3 s^{-1} [6].

CHARGE EXCHANGE (CXS) REACTIONS

The CXS rate coefficient for D is, as already mentioned in [7], a factor of 2 larger than the rate for He in the T_e range between 2eV and 15eV. But the difference in CXS alone cannot explain the difference in the detachment mechanisms.

NEUTRAL IONISATION

The larger mean-free-path (λ^{mfp}) for He^0 ionisation (the rate coefficient for ionisation of D is factor of 24.6 larger than for He at $T_e = 10$eV) allows He neutrals to escape from the divertor region to the X-point region. The power loss due to strong He radiation (mostly from He^+) leads to a particle flux detachment (the energy is not sufficient for ionisation of the recycled neutrals) [4,7].

The Fig.2 shows clear the movement of total radiation from the inner divertor to the region above X-point. The HeII emission shows a similar behaviour as the total radiation. Initially located at both inner and outer strike zones at low density, the total and HeII-radiations increasingly concentrates at the inner leg (broad distribution in total and HeII radiation in inner leg) and then take off from the inner target and move to the X-point.

This strong correlation lets assume that the total radiation is coming mostly from He^+ and He^0 . This assumption is fully consistent with B2.5-Eirene calculations [7]. Additionally the new EDGE2D-simulations came to same result and shows that the contribution from C is lower than 4% at high density. The comparison between simulation of total radiated power distribution and measured ones is given in figures 4 and 5 (c1,c2) and shows a good agreement.

To understand the emission distribution (D_α, HeI, HeII, CIII) in deuterium and helium plasmas the EDGE2D/NIMBUS code was used. Poloidally and radially uniform transport coefficients were $D_\perp = 0.2m^2/s$ and $\chi_\perp = 1m^2/s$ for particle and energy respectively. Simulations with these coefficients produced good matches for deuterium and helium plasmas with measured edge radial profile and temperature (edge LIDAR Thomson scattering). Fig.3 shows edge ne profiles compared with various diagnostics (Li beam diagnostic, edge and core LIDAR Thomson scattering) for two different central average electron densities in deuterium (Fig.3(a)) and helium (Fig.3(b)) plasmas. Additionally, a good correlation

between measured and calculated Te at strike points was observed (deviations are below diagnostic accuracy at low T_e) Figures 4 and 5 show the simulated and observed emission pattern in the divertor MkIIGB for two different central averaged densities in deuterium (Fig.4) and helium (Fig.5) discharges. 2D-emission profiles correlate well with EDGE2D calculations. The code simulates a similar behaviour for D_α -emission: emission begins at the inner and switches to outer divertor at high ne. The increase of D_α -emission in the outer leg at high ne can be explained by decreasing of outer leg electron temperature. The ratio of ionisation per photon for D_α, the so-called S/XB-value, decreases by a factor of 2.7 (from 38 ($T_e = 18$ eV) to 14 ($T_e = 4$ eV) [5]), thereby indicating an actual increase of a factor of 2.7 for the Da-emission, due to excitation only. Possible changes in the proportion of molecular deuterium have not been taken into account in this first approximation (see, for instance, [8] for details on suitable corrections). Also the CIII asymmetry was simulated with EDGE2D code. The measured and calculated CIII-radiation is much stronger in the outer divertor, with an additional significant contribution near the X-point. Also the observed reduction of CIII with ne increasing was simulated with code. The spatial contribution of HeI (706nm) emission is, in the early discharge phase, nearly symmetrical (the calculations show a reasonable radiation in the outer leg, but it cannot explain completely the symmetry observed in the experiment). It rapidly increases in the inner divertor during the density rise (see Fig.5(d2)). One sees that the simulated HeI emission patterns match the measured ones well during the later discharge phase. On the other hand, the simulation shows a poor correlation between simulated HeII(468nm) and measured ones. At high ne the measured HeII-emission shows, in contradiction to simulations, significantly more radiation from the inner leg than from the outer. The simulated T_e (calculated $T_e = 1.5$eV at inner strike point; the probes measure the value of 3eV,which however overestimates Te because of interpretation difficulties of the I-V characteristics in this regime) in the inner leg is possibly lower than in reality. In the T_e range around 2eV even slightly underestimation of Te leads to strong increase of λ^{mfp} for He^0 ionisation ($sn(T_e = 2eV)/sn(T_e = 1.5eV) \gg 30$) and correspondly moves the simulated ionisa-tion front away from the target. That leads to the reduction of simulated He + concentration in the inner leg and, accordingly, to the decrease of HeII emission. Calculations show that the major contributing process to emissions is excitation. The direct contribution from charge-exchanges (but it nevertheless can significantly influence the ionisation balance of carbon [2] and thus was included in the EDGE2D calculations) and recombination's is below of 5% from excitation and play insignificant role in the total radiation.

REFERENCES

[1] J. Rapp, A. Huber, L.C. Ingesson et al., J.Nucl. Mater. 313-316 (2003) 524

[2] A. Huber, P.Coad, D.Coster et al., J.Nucl. Mater. 313-316 (2003) 925

[3] A. Loarte et al., Nucl. Fusion 38 (1998) 331.

[4] R. Pitts, P. Andrew, Y. Andrew et al., J.Nucl. Mater. 313-316 (2003) 777

[5] H.P. Summers, ADAS User,s Manual, Rep. IR(94) 06 JET Joint Undertaking, Abingdon

[6] S.I. Krasheninnikov, A.Yu. Pigarov, D.A.Knoll et al., Phys Plasmas 4 (1997) 1638

[7] M. Wischmeier, D. Coster, X. Bonnin et al., J.Nucl. Mater. 313-316 (2003) 980

[8] Ph. Mertens et al., Plasma Phys. Control. Fusion 43 (2001) A349

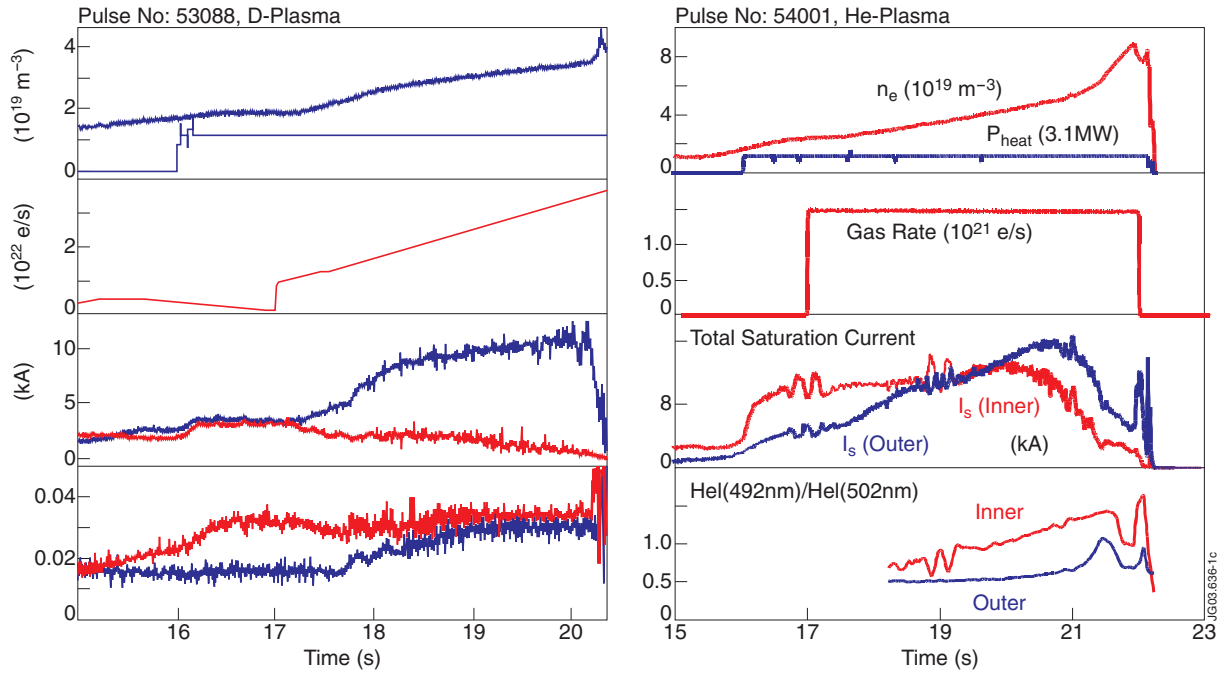

Figure 1: Time evolution of a typical deuterim (left) and helium (right) L-mode, density limit discharges in JET with the MkIIGB divertor.

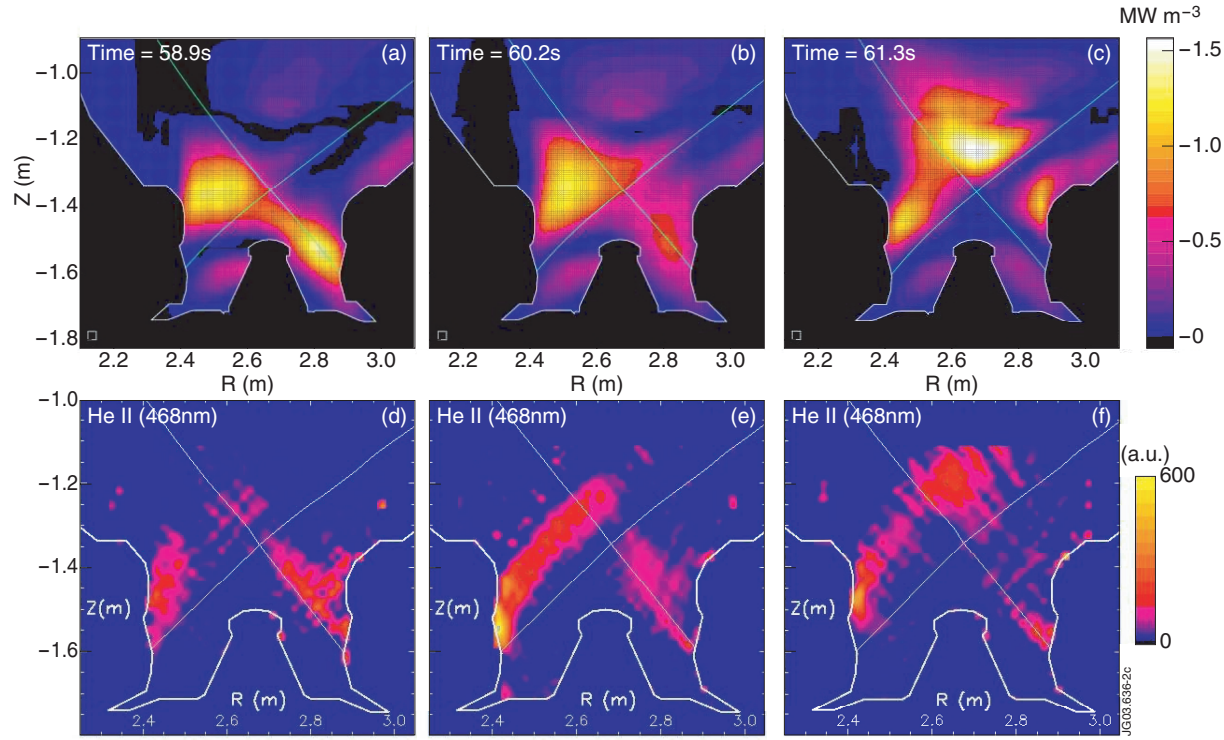

Figure 2: Total radiated power (top) and HeII-emission (bottom) in the divertor during three phases of the He L-mode density limit discharge (Pulse No: 54001)

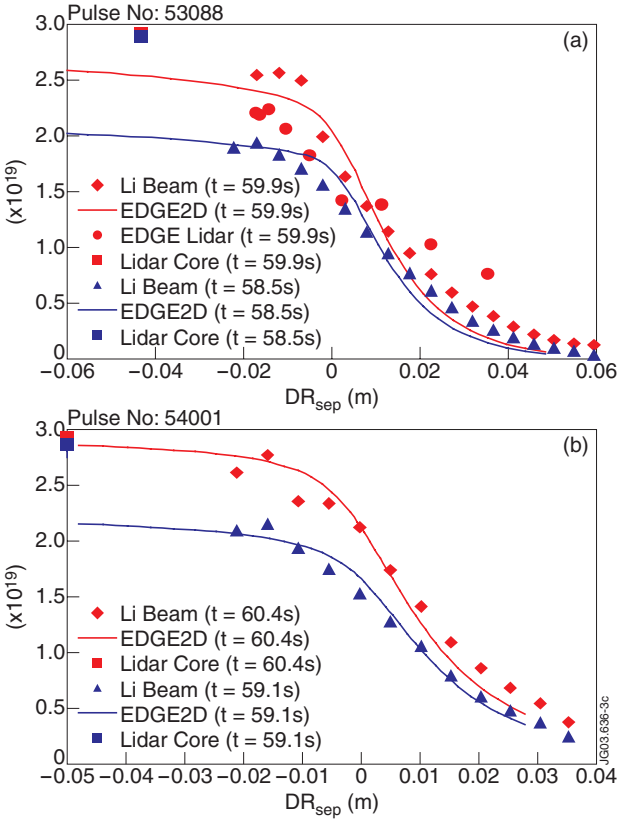

Figure 3: Edge profiles for D (a) and He (b) discharges from EDGDE2D compared with various diagnostics

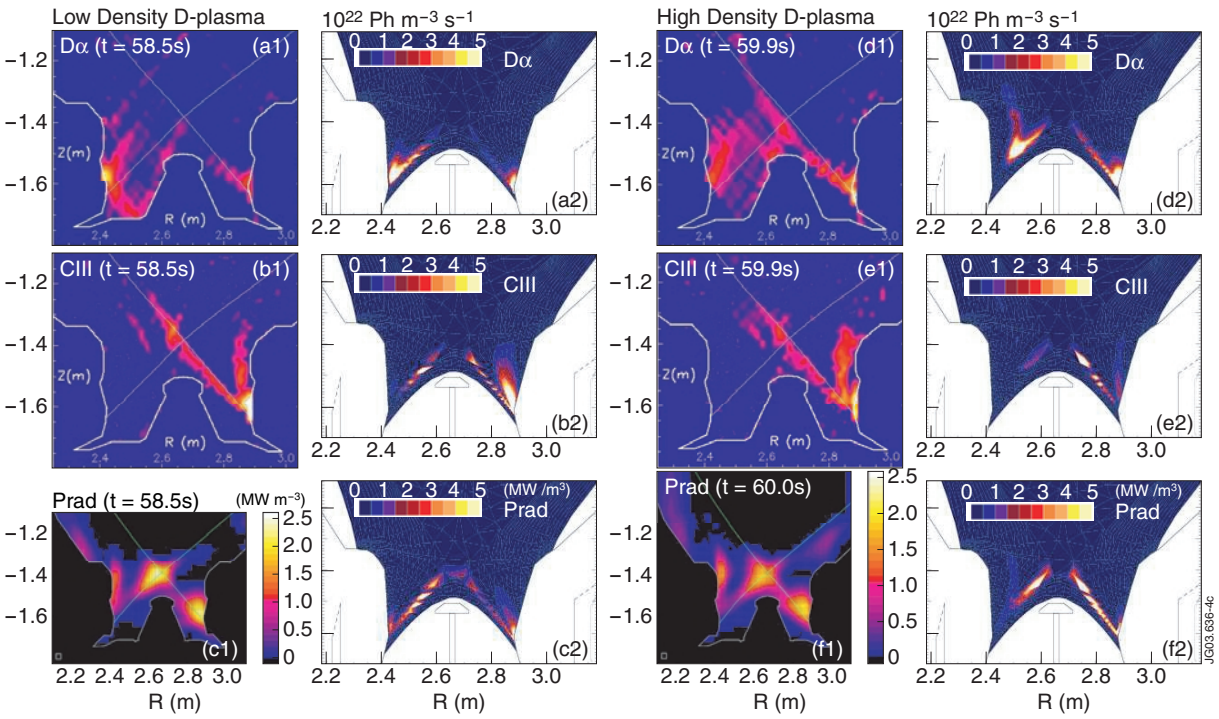

Figure 4: Simulated (a2,b2,c2,,d2,e2,f2) and observed (a1,b1,c1,d1,e1,f1) emission pattern in the divertor MkIIGB of JET during deuterium L-mode density limit discharge (Pulse No: 53088)

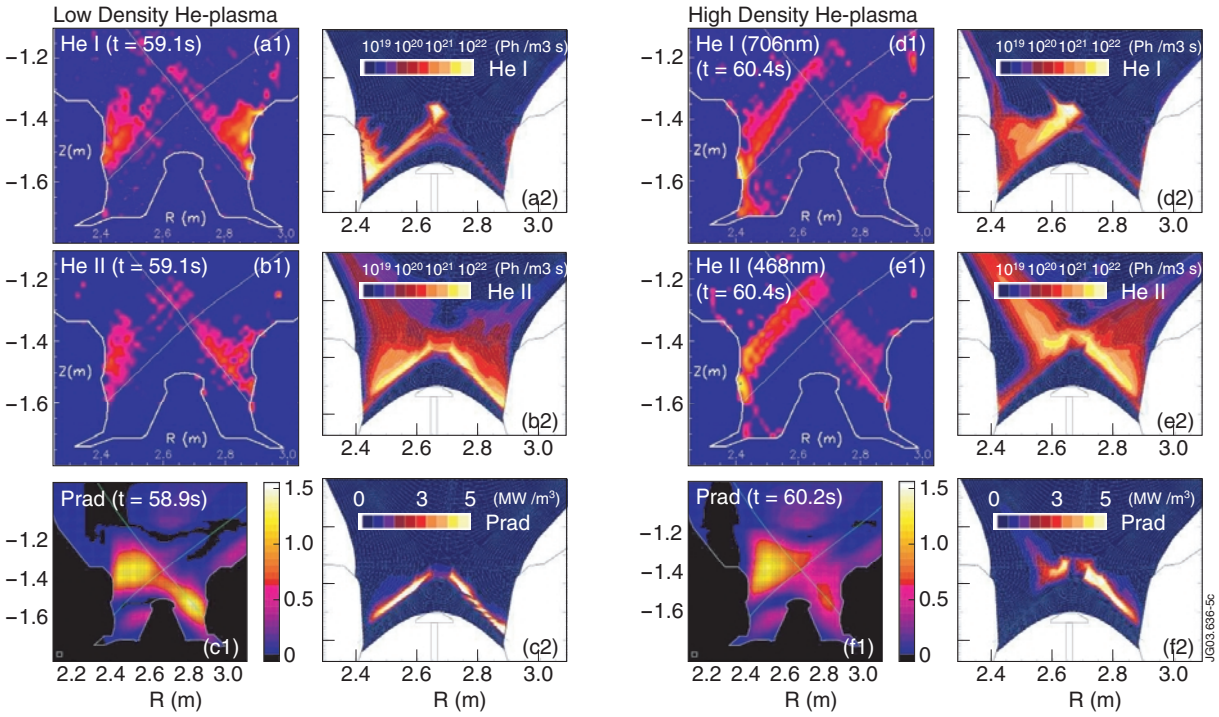

Figure 5: Simulated (a2,b2,c2,,d2,e2,f2) and observed (a1,b1,c1,d1,e1,f1) emission pattern in the divertor MkIIGB of JET during helium L-mode density limit discharge (Pulse No: 54001)